Land-ice studies

Studies of the west antarctic ice sheet, 1996–1997

C.R. BENTLEY, M.D. STENOIEN, S. SHABTAIE, C. LIU, *and* N. LORD, *Geophysical and Polar Research Center, University of Wisconsin, Madison, Wisconsin 53706*

Fieldwork

Airborne collection of remote-sensing data over the "Trunk D" area, comprising ice stream D, the adjacent ridges, and portions of ice streams C and E, was conducted by the Support Office for Aerogeophysical Research (SOAR) between 9 December 1996 and 16 January 1997. We at the University of Wisconsin will be analyzing the radar-sounding and laser-altimeter data over a subset of the area (figure 1).

Clouds were the main obstacle to collecting laser-altimeter data; the surface return was obscured to some degree on 60 percent of the flights. Where the laser was blocked by clouds, the terrain clearance will be determined (to a lesser accuracy) from the radar soundings.

Over the UW area (figure 1) the ice thickness varies from 500 to 2,000 meters (m), well within the range of the SOAR 60-megahertz (MHz) ice-sounding radar. On the interstream ridges (including Siple Dome), where there is little surface scattering, the bottom echo is mostly strong and internal layers clear (figure 2). Surface clutter, however, totally masks the bottom echo over the ice-stream margins and interferes seriously with it elsewhere over the ice stream. Internal layers either are not present in the ice stream or are completely masked by the surface scatter.

Fading pattern experiments

Radar signals returning from the irregular surfaces in and under the ice are modified by diffraction. Consequently, when the radar system is moved across the snow surface, the form of the returning signal changes rapidly, producing the spatial "fading pattern." Repeated measurements of the fading pattern can reveal the relative displacement between the snow surface and the reflecting horizons.

Six grids near station Upstream B on ice stream B2 were surveyed with a digital 50-MHz ice-sounding radar two or three times each during the 1991–1992 field season (Bentley et al. 1992). Grids measured several hundred meters across; the spacing between lines was 30 or 50 m. The grids were defined by bamboo stakes emplaced at close, precisely positioned intervals.

The radar system was towed by a Tucker Sno-Cat at a speed of approximately 8 kilometers per hour. An automated system, comprising a microcontroller and a trailing bicycle wheel, triggered the radar system every 0.7 meters. A microwave motion sensor that detected

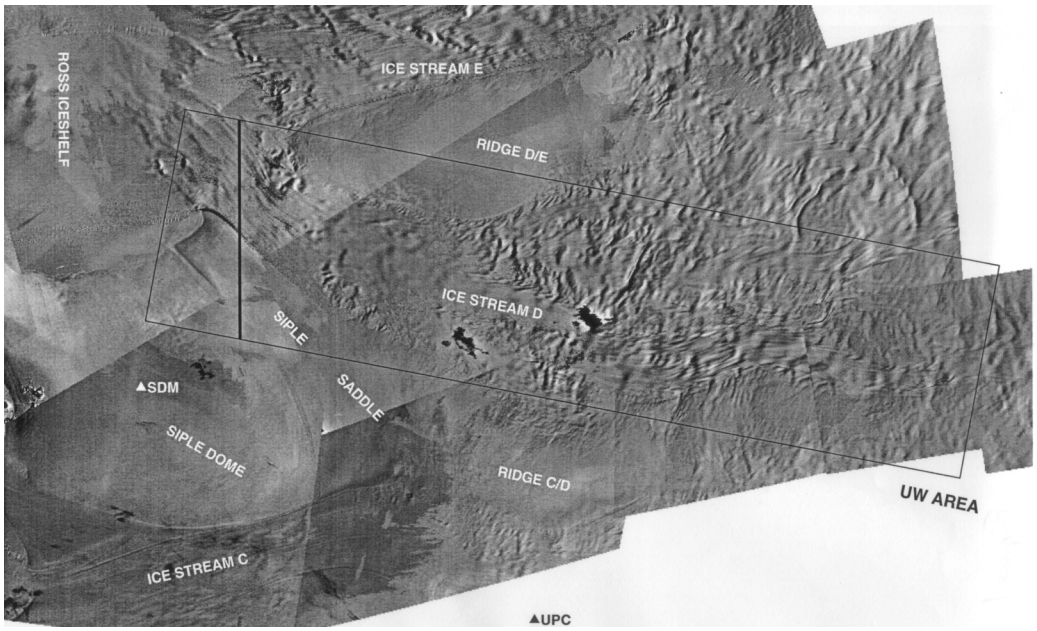

Figure 1. Location map of the University of Wisconsin survey area over ice stream D. The satellite-image base map is from P.L. Vornberger and R.A. Bindschadler (personal communication). North is toward the upper left corner. Triangles denote surface camps "Siple Dome" (SDM) and "Upstream C" (UPC). Flow in the ice streams is from right to left. The box shows only the margins of the UW block; the grid of individual flight lines covers the block at 5-kilometer intervals in both directions. The heavy line denotes the location of the section in figure 2.

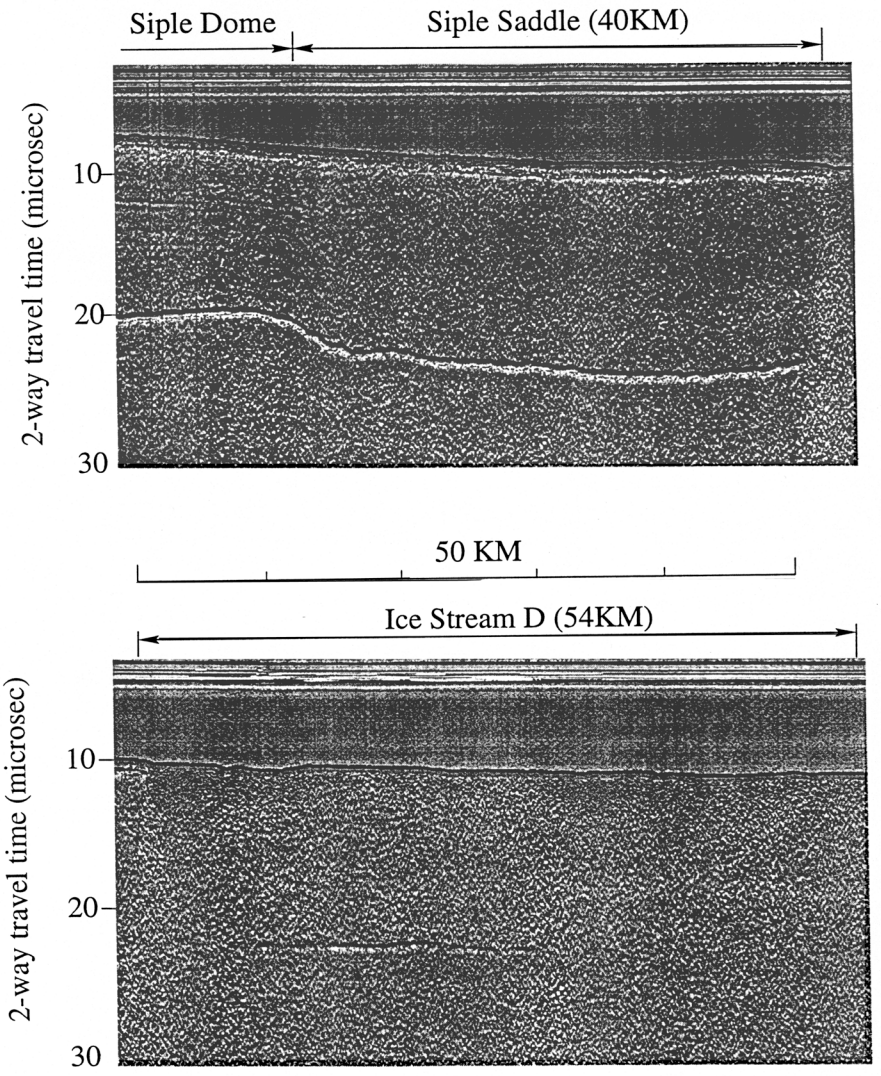

Figure 2. Radargrams from the 1996–1997 field season over the UW area (see figure 1 for the location). The section continues from upper left to lower right, with a slight overlap to aid in the visual connection between the two halves. Travel times are round-trip from the aircraft. The reflection at 8–10 microseconds is from the surface; that at 20–22 microseconds is from the bed.

the stakes and a manual trigger provided registration marks on the digital record.

The data spacing was not constant because

- the surface snow conditions varied with time and place, so the spatial interval between outgoing pulses from the bicycle wheel was not constant;
- a trace was lost whenever a flag was marked manually; and
- occasionally, traces were lost for some other reason.

Therefore, to facilitate an analytical comparison of fading patterns, the originally recorded amplitude and phase were resampled at a constant spatial interval by interpolation between adjacent traces.

The amplitude and phase of the resampled fading patterns were compared analytically through cross-correlation analysis to estimate the displacement between surveys. The phase data were first unwrapped and filtered to remove initial phase differences and the effect of the ice-thickness gradient. The internal returns were used to remove the positioning error of the antennas, whose distance from the motion detector varied slightly from survey to survey—we equated the displacement between the apparent fading patterns from the bed and from selected internal horizons in the upper 70 percent of the ice (which we assume is not deforming) to the displacement between the surface and the bed.

Completed results at one of the grids from two sets of independent measurements over consecutive time intervals of 24 and 27 days, show that the basal irregularities travel 0.3±1.0 meter per year more slowly than the surface. Thus, at least 99.7 percent of the ice-stream movement of 440 meters per year (Whillans, Bolzan, and Shabtaie 1987) takes place by sliding and/or bed deformation; no more than 0.3 percent occurs by shear straining within the ice.

Satellite radar altimetry and InSAR

Work continues on two projects that use satellite-based active microwave sensors to view the west antarctic ice sheet.

- In our topographic-estimation project, we combined radar-altimeter data from the European Space Agency's ERS-1 remote-sensing satellite and a newly developed 3-dimensional inversion algorithm to map the kilometer-scale topography of ice streams D and E and Pine Island and Thwaites Glaciers. A comparison with 385 global positioning system (GPS) position and height measurements in the catchment area of ice stream D (Bindschadler 1997; Bindschadler, Chen, and Vornberger, *Antarctic Journal*, in this issue) yields a standard deviation in the mapped height of about 6 meters.
- Our interferometric synthetic aperture radar (InSAR) experiments are focused on the problems of applying InSAR to the slow-moving interior of the Pine Island Glacier catchment area, far from any known stationary points. We have begun to produce interferograms; their analysis in terms of ice-sheet elevation and motion is in its early stages.

Interpretive studies: Saddle zones

The ice sheet of West Antarctica is conventionally divided morphologically into four classes with differing ice dynamics: the interior ice sheet, ice streams, domes, and ridges. There is, however, a fifth class that should be recognized—ice-sheet saddle zones, which lie between the domes, ridges, and ice streams.

An example is "Siple Saddle," which separates Siple Ice Dome from ridge C/D (figure 1). Radar soundings across the boundary between Siple Saddle and Siple Dome (figure 2) reveal no sign of an active or relict ice-stream margin there; although there is a slight increase in crevasse scatter over the saddle, it is strikingly less than that over the margin of ice stream D (figure 2) or C (Shabtaie and Bentley 1987). Instead, the radar data show a saddle in ice elevation; the surface profile is concave up between Siple Dome and ridge C/D and concave down between ice streams C and D. Satellite imagery of this area shows several curvilinear undulations in height within the saddle zone, running from ice stream C to ice stream D. We interpret those features to indicate that the saddle is currently widening both toward ridge C/D and toward Siple Dome. We believe that "Siple Saddle" is dynamically active and not in equilibrium.

This work was supported by National Science Foundation grants OPP 92-22092 and OPP 93-19043 and National Aeronautics and Space Administration contract NAS5-33015. (Contribution number 580 of the Geophysical and Polar Research Center, University of Wisconsin at Madison.)

References

Bentley, C.R., A.N. Novick, N. Lord, T.S. Clarke, C. Liu, Y.Y. Macheret, and A.N. Babenko. 1992. Radar experiments on ice stream B. *Antarctic Journal of the U.S.*, 27(5), 43–44.

Bindschadler, R.A. 1997. Determination of velocity field and strain-rate field in West Antarctica using high precision GPS measurements. Paper presented at West Antarctic Ice Sheet Initiative Meeting, Washington D.C., September 1997.

Bindschadler, R.A., X. Chen, and P.L. Vornberger. 1997. Surface velocity and strain rates at the onset of ice stream D, West Antarctica. *Antarctic Journal of the U.S*, 32(5).

Shabtaie, S., and C.R. Bentley. 1987. West antarctic ice streams draining into the Ross Ice Shelf: Configuration and mass balance. *Journal of Geophysical Research*, 92(B2), 1311–1336.

Vornberger, P.L., and R.A. Bindschadler. 1997. Personal communication.

Whillans, I.M., J. Bolzan, and S. Shabtaie. 1987. Velocity of ice streams B and C, Antarctica. *Journal of Geophysical Research*, 92(B9), 8895–8902.

Surface velocity and strain rates at the onset of ice stream D, West Antarctica

ROBERT A. BINDSCHADLER, *National Aeronautics and Space Administration, Goddard Space Flight Center, Greenbelt, Maryland 20771*

XIN CHEN *and* PATRICIA L. VORNBERGER, *General Sciences Corporation, Laurel, Maryland 20727*

Ice streams are the rapidly moving conveyors of ice that drain the majority of ice in West Antarctica. Their behavior holds the key to the ice sheet's future, yet it remains unknown why they occur where they do. Investigations focused on the crevassed margins, the lubricated bases, the entrances into the floating ice shelves as well as the trunk of the ice streams have greatly increased our understanding of how an ice stream moves and changes, but very little attention has been directed toward the areas where ice streams begin (Anandakrishnan et al. in press).

Landsat imagery shows flow features that suggest ice stream D begins in a relatively narrow region close to Byrd Sur-

face Camp. This situation made it our preferred choice for a survey of the surface velocity and deformation field. Ice flow at Byrd was approximated to be 13 meters per year (m/yr) (Whillans 1979). We later measured it to be only 11 m/yr, and with repeat imagery, we tracked the motion of a crevasse 160 kilometers (km) downstream at 130 m/yr, so our survey grid was designed to cover this at a 5-km spacing and a width that varied from 60 km upstream to 30 km downstream. Our primary objective was to locate the onset region and characterize the ice flow and deformation in its vicinity.

Surface surveys were conducted November to December of 1995 and 1996 by traversing the area with a mobile camp supporting a field team of five. Snowmobiles were used to establish each site and global positioning system (GPS) receivers used to collect data at each site in both years. The grid was surveyed in a series of 11 blocks. A GPS base station at the mobile camp centered within each block provided a precise position from which each surrounding grid site could be located by differential baseline analysis of the GPS data. Data were processed daily to ensure data integrity, and when necessary, measurements were repeated. Multiple observations at sites shared at block boundaries demonstrated that survey precision was 8.5 centimeters horizontally and 15 centimeters vertically (Chen, Bindschadler, and Vornberger in press).

Figure 1 shows the measured velocity vectors. It demonstrates that the major flow enters the grid south of Byrd flowing westward and turns to the southwest as it accelerates. This direction follows a subglacial trough averaging roughly 950 meters below sea level indicating that subglacial relief exerts a major influence on the direction of streaming flow in this area (Bamber and Bindschadler in press).

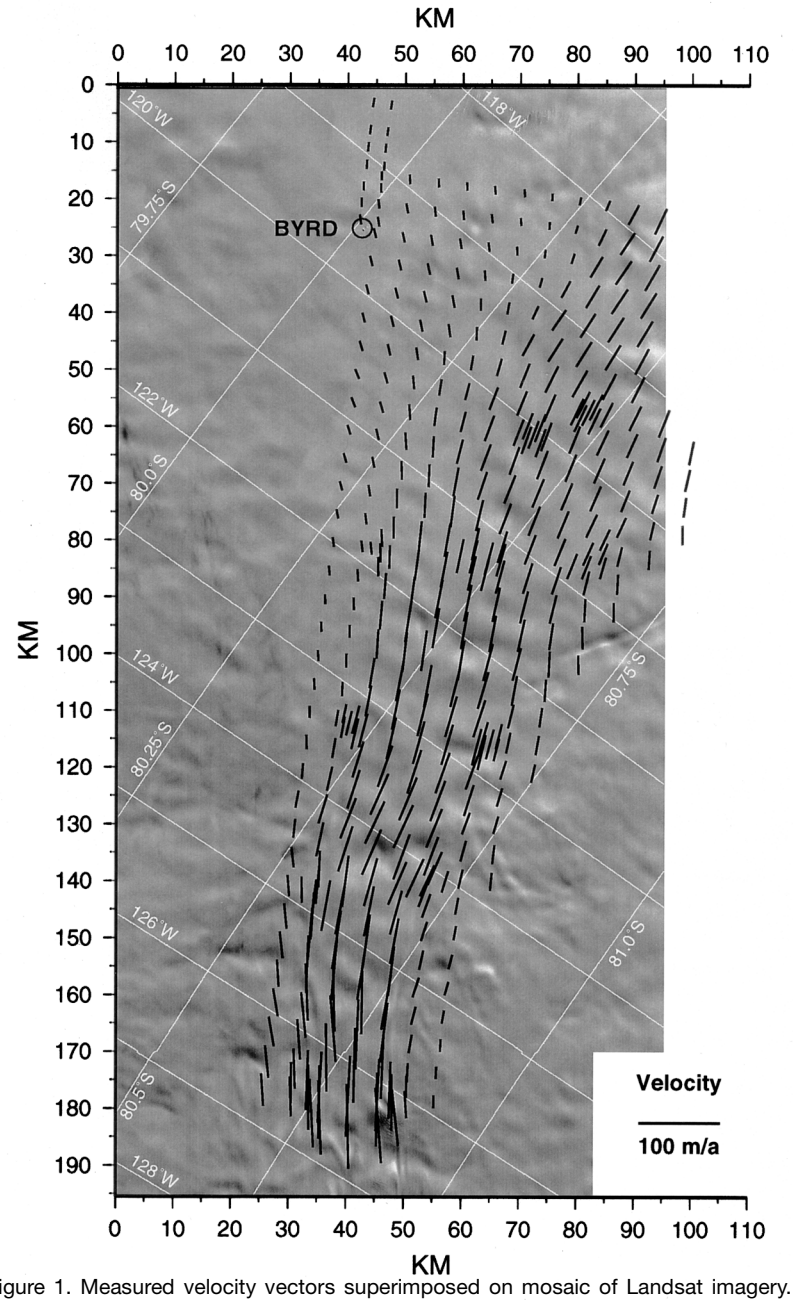

Figure 1. Measured velocity vectors superimposed on mosaic of Landsat imagery.

Figure 2 shows the surface strain-rate field. The increasing shear at the margins of the developing ice stream is clearly represented. Not shown is the strain-rate field measured upstream of Byrd at sites first established as part of the Byrd Station Strain Network (BSSN) (Whillans 1979). Our strain measurements were identical to the BSSN measurements collected between 1963 and 1967 indicating no change in the deformation field over more than 30 years.

The region of shear near the grid's upstream end is particularly interesting because it occurs where a series of flowlines originates, which themselves run obliquely to the measured flow direction. This region is believed to be undergoing change.

Based on our observations and analysis of the driving forces exerted on the ice, we identify the onset of ice stream D as near the downstream end of our grid (at approximately the 125 km coordinate in figure 1).

This research was supported by National Science Foundation grant OPP 93-17627.

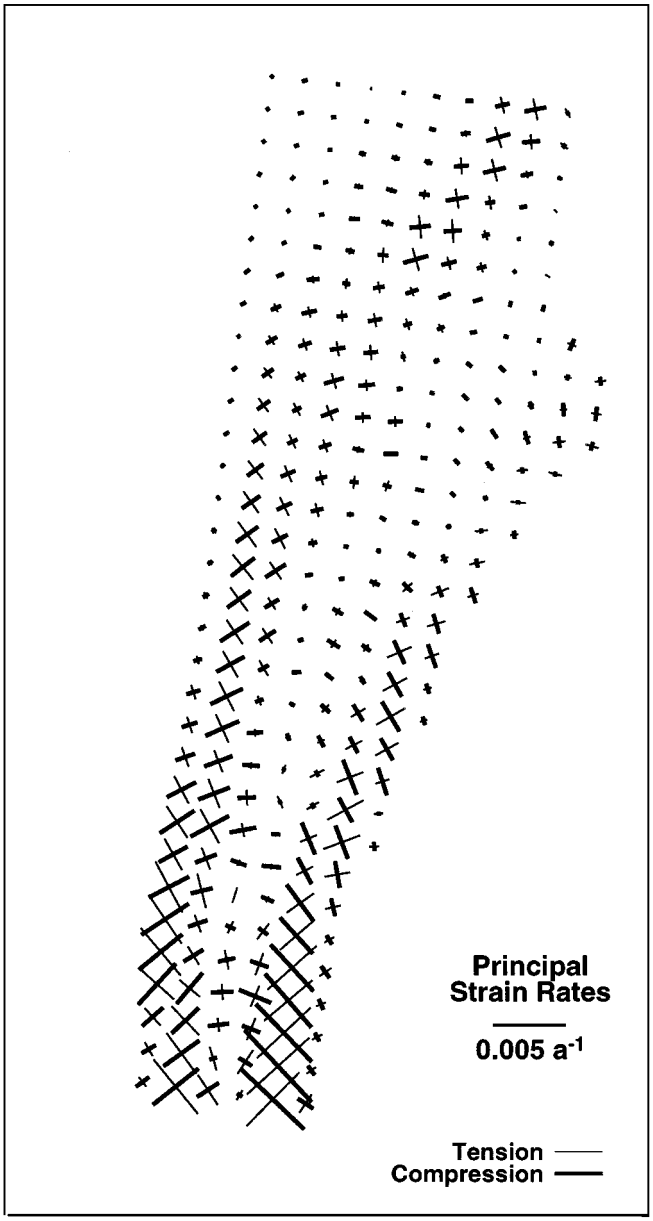

Figure 2. Strain rates calculated from velocity field. Fine lines are principal tension; heavy lines are principal compression. (a^{-1} denotes per year.)

References

Anandakrishnan, S., D.D. Blankenship, R.B. Alley, and P.L. Stoffa. In press. Geologic constraints on the flow-margin of a west antarctic ice stream. *Nature*.

Bamber, J.L., and R.A. Bindschadler. In press. An improved elevation data set for climate and paleo-climatic modeling: Validation with satellite imagery. *Annals of Glaciology*.

Chen, X., R.A. Bindschadler, and P.L. Vornberger. In press. Determination of velocity field and strain-rate field in West Antarctica using high precision GPS measurements. *GPS Journal*.

Whillans, I.M. 1979. Ice flow along the Byrd Station Strain Network, Antarctica. *Journal of Glaciology*, 24(90), 15–28.

Visible examination of Siple Dome, West Antarctica, shallow cores

RICHARD B. ALLEY, MATTHEW K. SPENCER, *and* DONALD E. VOIGT, *Earth System Science Center* and *Department of Geosciences, Pennsylvania State University, University Park, Pennsylvania 16802*

Nine shallow cores were collected in a transect across Siple Dome during the 1996–1997 field season by the Polar Ice Coring Office, Lincoln, Nebraska, and the WAISCORES (West Antarctic Ice Sheet Cores) Science Coordination Office, Reno, Nevada. These cores were analyzed by many WAISCORES investigators at the National Ice Core Laboratory, Denver, Colorado, during the summer of 1997. As part of this analysis, all cores were examined visually, and many were thin sectioned by investigators in our team from Penn State. Optical analyses were also conducted by Kendrick Taylor, Desert Research Institute, Reno, Nevada, and some cores were examined visually by Tony Gow and Debra Meese of the U.S. Army Cold Regions Research and Engineering Laboratory, Hanover, New Hampshire. Thin-section analyses and some visible examinations were also conducted by Joan Fitzpatrick, U.S. Geological Survey, Denver, Colorado.

The "typical" visible annual signal of summertime depth hoar and finer-grained, denser wintertime accumulation is present (*see* Alley and Bentley 1988). The relatively low accumulation rate (approximately 0.12 meter of ice per year, based on our preliminary dating) complicates interpretation somewhat; accumulation from a prominent storm is potentially a significant fraction of a year, so storm-related features may mimic annual features, and vice versa. It is also possible that "depositional depth hoars" are present owing to odd wintertime weather patterns. Repeated counting of layers by one investigator and comparisons among investigators indicate that our identification of annual layers is reproducible to better than 10 percent but not at the 1 percent level found in optimal cores. Comparison to preliminary data graciously advanced by other WAISCORES investigators indicates that our reproducibility may be close to our accuracy, although further work remains.

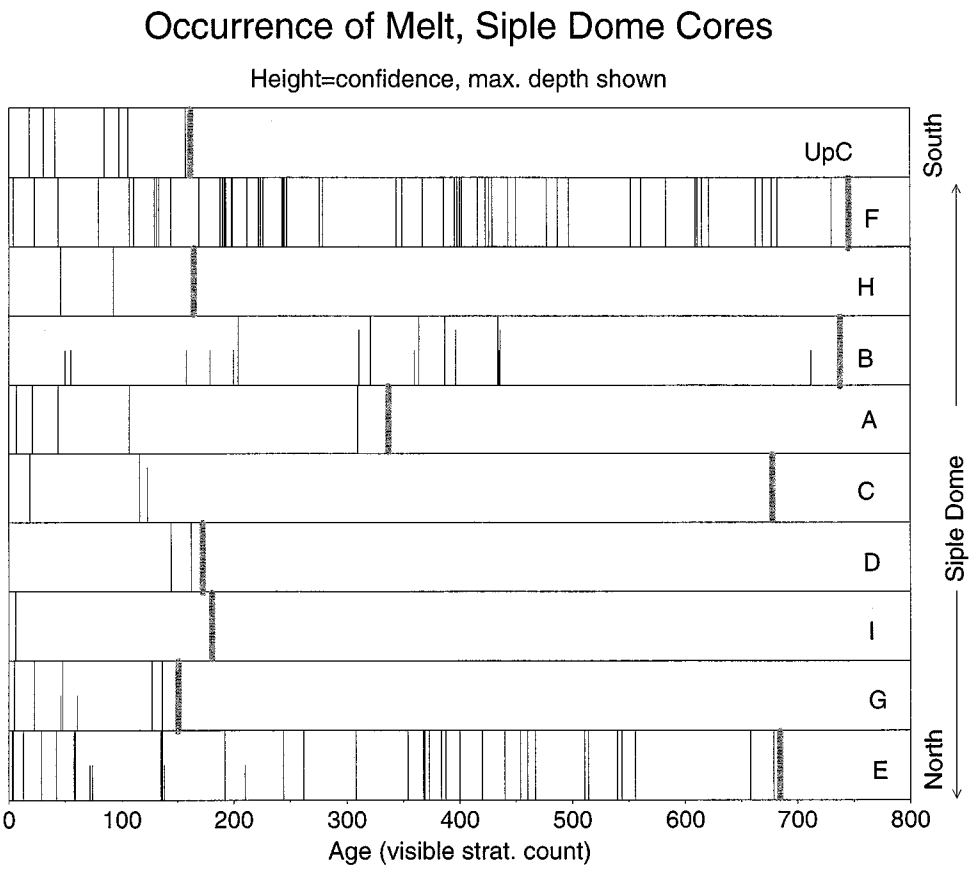

Figure 1. Occurrence of melt layers in the Siple Dome cores, and in the Upstream C (UpC) core from ice stream C, arranged from south (top) to north (bottom); the WAISCORES identification code for each core (A-I and UpC) is indicated. Most melt layers were unequivocally identifiable and are shown with a vertical bar. Those that might have been mistaken for a crust (a thinner bubble-free feature that may arise from melt, wind packing, or other processes) are indicated by shorter bars. Dating is preliminary and based on visible-stratigraphic identification of summer layers by Penn State researchers. The bottom of each core is indicated by the thick, patterned line. In the case of Upstream C, the core continued below the patterned line shown, but layering was badly disturbed; we identify the onset of disturbance as approximately the time when ice stream C ceased moving rapidly.

Among the features visible in the cores are melt layers. Occurrence of melt layers at similar depths and ages in many different cores probably indicates that the records of major melt events are sufficiently widespread and continuous to provide time horizons, although some discontinuity is indicated by failure of prominent layers to appear in certain cores. Improved dating should allow further testing of these results. The occurrence of melt layers in the cores is shown in figure 1, arranged as a transect

across Siple Dome from south to north; cores near the crest of the dome are plotted in the middle of the figure. Data also are included from a core farther south at Upstream C on ice stream C (82°26'S 135°58'W, altitude 506.25 meters). Only the upper 30 meters of the Upstream C core are shown, because deeper layers in that core appear disturbed. Clear variation in melt frequency is apparent and quantified in figure 2.

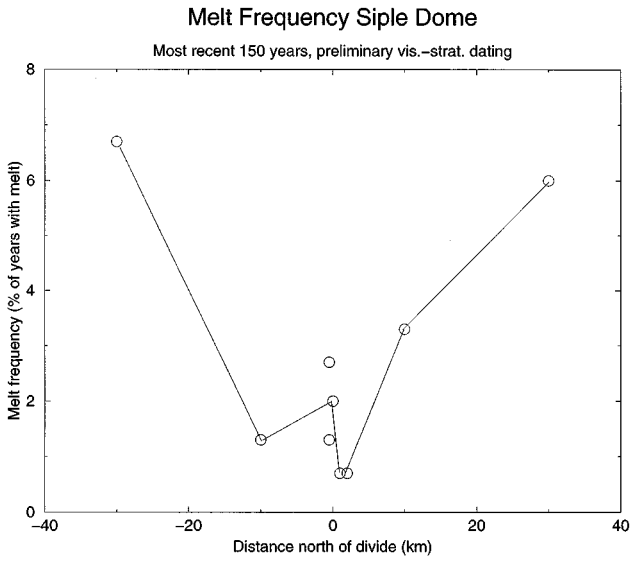

Figure 2. Frequency of melt occurrence for the Siple Dome cores, as a function of position from south to north across the dome. The most recent 150 years were used for the calculation in all cases, so that this represents spatial variability rather than time trends. (vis.-strat. denotes visible-stratigraphic.)

Over the most recent 150 years, based on our preliminary dating, melt occurs in between 0.7 percent and 6.7 percent of years in the Siple Dome cores and in 4.7 percent of the years at Upstream C. Notice that most of the accumulation from years containing melt features is ordinary, unmelted firn. This occurrence is not so frequent that it is likely to compromise other paleoclimatic measurements, especially because the melt layers are easily recognized and avoided in sampling for proxies that might be affected by melt. The lower frequency of melt near the crest of the dome almost certainly is related to its higher elevation.

Further statistical analyses are required (cf. Alley and Anandakrishnan 1995), but it appears that melt occurence has time trends. Interesting patterns, including a possible biannual signal at some ages in the lower elevation cores, also occur. Based on previous work relating melt occurrence to summertime warmth (Zwally and Fiegles 1994), we expect that the melt frequency can be used as a paleothermometer for summertime conditions.

This research was supported by National Science Foundation grants OPP 95-26374 and OPP 94-17848. We thank Todd Dupont and Byron Parizek for "field" work, at the National Ice Core Laboratory, and the WAISCORES Science Coordination Office, the National Ice Core Laboratory, the Polar Ice Coring Office, and WAISCORES colleagues.

References

Alley, R.B., and S. Anandakrishnan. 1995. Variations in melt-layer frequency in the GISP2 ice core: Implications for Holocene summer temperatures in central Greenland. *Annals of Glaciology*, 21, 64–70.

Alley, R.B., and C.R. Bentley. 1988. Ice-core analysis on the Siple Coast of West Antarctica. *Annals of Glaciology*, 11, 1–7.

Zwally, H.J., and S. Fiegles. 1994. Extent and duration of antarctic surface melting. *Journal of Glaciology*, 40(136), 463–476.

Glaciochemical studies at Siple Dome, West Antarctica, during the 1996–1997 season

KARL J. KREUTZ, PAUL A. MAYEWSKI, MARK S. TWICKLER, *and* SALLIE I. WHITLOW, *Climate Change Research Center, Institute for the Study of Earth, Oceans, and Space* and *Department of Earth Sciences, University of New Hampshire, Durham, New Hampshire 03824*

L. DAVID MEEKER, *Climate Change Research Center, Institute for the Study of Earth, Oceans, and Space* and *Department of Mathematics, University of New Hampshire, Durham, New Hampshire 03824.*

Deep ice cores collected from the interior of the west antarctic ice sheet and the interice stream ridges along the Siple Coast potentially contain long time-series records of Southern Hemisphere environmental change. One such location is Siple Dome, an approximately 120-kilometer (km) × 250-km ice dome located between ice streams C and D (figure 1). Because of promising results from reconnaissance glaciochemical (Mayewski, Twickler, and Whitlow 1995) and geophysical (Raymond et al. 1995) research, current U.S. deep ice-coring efforts are focused in the area. Drilling at Siple Dome is advantageous for several reasons, including the site's relatively simple geometry and internal layering (Raymond et al. 1995) and its sensitivity to changes in South Pacific lower atmospheric circulation (Kreutz and Mayewski in press). Changes in the strength of these circulation conditions over the last millennium have been documented using glaciochemical measurements from a 150-meter (m) ice core collected at Siple Dome in 1994 (Kreutz et al. 1997). As part of the U.S. WAISCORES program, the approximately 1,000-m ice core recovered from Siple Dome will extend such well-dated, multiparameter, high-resolution environmental reconstructions back about 100,000 years and be used to investigate several issues, including

- local and regional climatic change through comparison with deep ice cores recovered from the west and east antarctic plateaus,
- the global timing and extent of rapid climate changes based on comparison with Greenland ice cores, and
- past west antarctic ice sheet ice dynamics and their impact on global sea level.

In preparation for the recovery, analysis, and interpretation of the Siple Dome deep core, a thorough understanding of the modern glaciochemical spatial variability in the area is essential. Spatial studies were begun during the 1994–1995 season, when five snowpits were collected on a 10-km × 10-km surveyed grid centered on the Siple Dome summit (Mayewski et al. 1995). Sampling during the 1996–1997 season expanded the glaciochemical spatial investigation completed in 1994–1995 and, in addition, collected clean surface snow and firn samples from the deep-core site. In addition to snowpits covering approximately 4–10 years of deposition, shallow (approximately 100-m) ice cores collected on the same spatial grid will allow investigation of modern and longer term changes in the spatial patterns of chemical deposition, source regions, moisture flux, and the relationship between glaciochemical and other measurements (e.g., stable isotopes and physical stratigraphy).

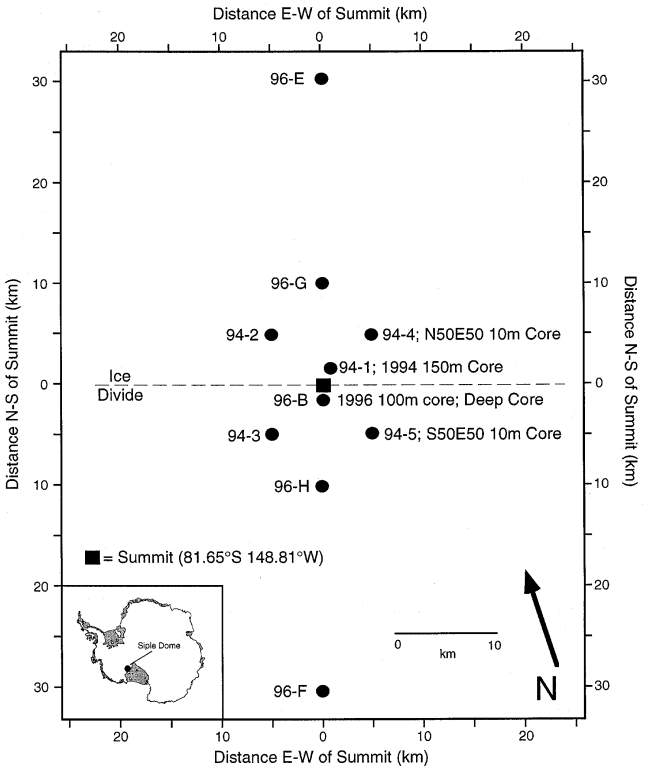

Figure 1. Location map for Siple Dome. Snowpits and cores collected during the 1994–1995 and 1996–1997 seasons are shown.

During the 1996–1997 season, four 2-m snowpits were sampled on a transect from 30 km north to 30 km south of the ice divide (figure 1). In addition, a 4-m snowpit and a 100-m, 10.16-centimeter-diameter ice core were collected approximately 0.5 km south of the summit, at the deep-core site (figure 1). All snowpit and core sample collection was performed by workers using nonparticulating suits, polyethylene gloves, and particle masks to avoid chemical contamination. Snowpits were sampled in conjunction with other investigators (C. Shuman, J. McConnell) so that all measurements are co-registered. The 100-m core is being sampled at high resolution (subannual sampling in the upper 15 m; biannual sampling in the bottom 85 m) to provide accurate firn measurements that

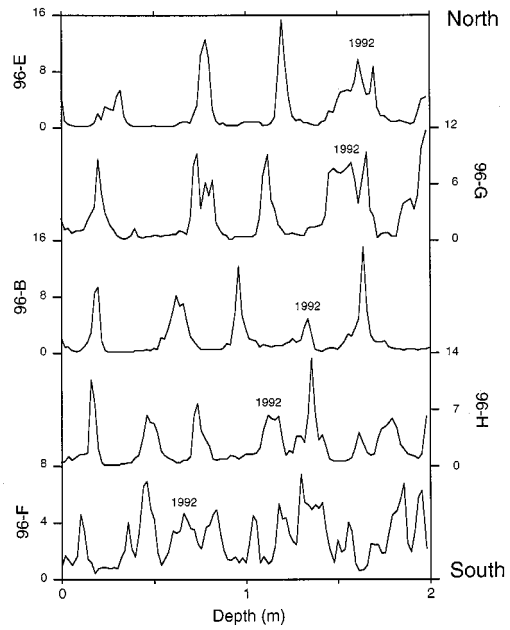

Figure 2. Measurements of $xsSO_4^=$ (in microequivalents per liter) in 1996–1997 Siple Dome snowpits. 96-B through 96-G refer to pit locations on figure 1.

overlap the deep core. Concentrations of major anions, cations [sodium (Na^+), calcium (Ca^{2+}), magnesium (Mg^{2+}), potassium (K^+), ammonium (NH_4^+), chloride (Cl^-), nitrate (NO_3^-), and sulfate ($SO_4^{2=}$)], and methanesulfonic acid (MSA; measured in core samples by the University of Miami) are measured via ion chromatography at the University of New Hampshire.

An example of the well-preserved glaciochemical signals present in the Siple Dome snowpack is given in figure 2. Concentrations of both excess (xs) $SO_4^=$ and MSA (both byproducts of the oxidation of phytoplankton-produced dimethylsulfide) peak in the summer in the antarctic atmosphere (Wagenbach 1996). Therefore, $xsSO_4^=$ maxima in the Siple Dome snowpack likely record peaks in summer biogenic activity. Such annual glaciochemical peaks can be used to assign dates to strata in snowpits (figure 2) and ice cores. Cores collected from Siple Dome thus far have been dated using a combination of high-resolution discrete chemical sampling, continuous measurements of Cl^-, NO_3^-, and liquid conductivity, and physical properties (Kreutz et al. 1997). This technique will be used in conjunction with other measurements (e.g., electrical conductivity, dielectric properties, and stable isotopes) to date the Siple Dome deep core.

Based on the dating technique outlined above, a gradient in the number of years contained in each snowpit along the 30-km north/30-km south transect over Siple Dome is apparent (figure 2). This gradient in years, likewise, suggests a gradient in accumulation rate (b) whose dominant moisture source is from the north. Average chemical concentration values for 1994–1995 and 1996–1997 pits are similar (Kreutz et al. in preparation); however, flux (concentration*b) calculations also show a distinct gradient in all species going from north to south across the dome (figure 3). It appears that the major source of marine [seasalt (ss) Na^+, MSA, and $xsSO_4^=$] species, like moisture, is from the north. This finding is consistent with previous work (Kreutz and Mayewski in press; Kreutz et al. 1997) and suggests the source of marine chemical species at Siple Dome is the Amundsen/Ross Sea region, with advection of lower tropospheric marine air across the Ross Ice Shelf to Siple Dome. Statistical investi-

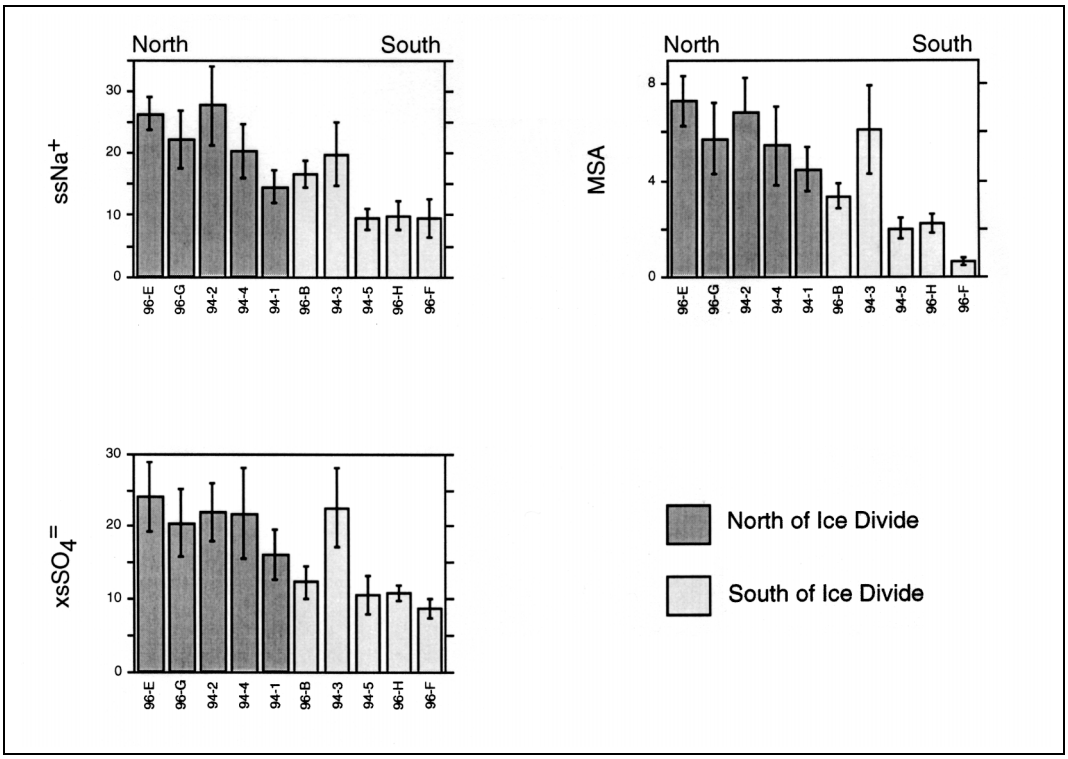

Figure 3. Mean annual chemical flux (in kilograms per square kilometer per year) in 1994–1995 and 1996–1997 Siple Dome snowpits (error bars represent standard error). The order of snowpits on the figure is along the transect from 30 km north (96-E) to 30 km south (96-F) of the ice divide. The method used to separate seasalt (ss) from nonseasalt [or excess (xs)] chemical fractions is given in Kreutz et al. (1997).

gation of glaciochemical variability on a range of spatial and temporal scales is currently being investigated (Kreutz et al. in preparation).

We thank our colleagues, the Siple Dome Science Coordination Office, Polar Ice Coring Office, Antarctic Support Associates, and U.S. Navy Squadron VXE-6 for field assistance at Siple Dome. This work was supported by National Science Foundation grant OPP 95-26449.

References

Kreutz, K.J., and P.A. Mayewski. In press. A basis for reconstructuring paleo-atmospheric circulation using west antarctic glaciochemical records. *Antarctic Science*.

Kreutz, K.J., P.A. Mayewski, L.D. Meeker, M.S. Twickler, S.I. Whitlow, and I.I. Pittalwala. 1997. Bipolar changes in atmospheric circulation during the Little Ice Age. *Science*, 277, 1294–1296.

Kreutz, K.J., P.A. Mayewski, M.S. Twickler, S.I. Whitlow, J.W.C. White, C.A. Shuman, C. Raymond, H. Conway, and N. Nereson. In preparation. Glaciochemical, isotopic, and stratigraphic properties of Siple Dome, Antarctica, surface snow.

Mayewski, P.A., M.S. Twickler, and S.I. Whitlow. 1995. The Siple Dome ice core-reconnaissance glaciochemistry. *Antarctic Journal of the U.S.*, 30(5), 85–87.

Raymond, C., N. Nereson, A. Gades, H. Conway, R. Jacobel, and T. Scambos. 1995. Geometry and stratigraphy of Siple Dome, Antarctica. *Antarctic Journal of the U.S.*, 30(5), 91–93.

Wagenbach, D. 1996. Coastal Antarctica: Atmospheric chemical composition and atmospheric transport. In E.W. Wolff and R.C. Bales (Eds.), *Chemical exchange between the atmosphere and polar snow* (NATO ASI Series, Vol. 43). New York: North Atlantic Treaty Organization.

Characterization of wind-generated snow surface features on the Ross Ice Shelf, Antarctica

JENNIFER STEWART, DAVID A. BRAATEN, *and* CAROLE BENNETT, *Department of Physics and Astronomy, University of Kansas, Lawrence, Kansas 66045*

A snow surface with mobile snow grains is essentially a sediment bed that is influenced by a turbulent air flow. The formation and evolution of snow surface features (e.g., ripples) caused by wind-driven snow grains have been previously examined and classified by Kobayashi and Ishida (1979). The impact of snow grains on the surface by saltation results in the formation of ripples (Kosugi, Nishimura, and Maeno 1992) as well as the liberation of small snow grains, which may be transported by suspension (Anderson and Hallet 1986). The dynamic processes of surface-feature formation display self similarity but are essentially nonlinear and chaotic processes (Tufillaro, Abbott, and Reilly 1992) in which the redistribution of snow grains forming snow-surface features distorts the turbulent flow, which in turn distorts the features.

Although cold-temperature wind-tunnel studies suggest that eolian snow ripples are comparable to corresponding ripples formed in other sediments such as sand (Kosugi et al. 1992), there are some differences in the observed morphology. An important difference between snow grains and sand grains is that snow grains are subject to interparticle cohesive forces and to sublimation during transport unlike sand grains (Schmidt 1986; Pomeroy and Gray 1990). Snow surface features are also hypothesized to play a role in near-surface ice-sheet ventilation processes known as wind pumping (Waddington, Cunningham, and Harder 1996) by the production of high-frequency, micropressure fluctuations caused by the turbulent air passing over the surface features.

A detailed characterization of snow surface features on the Ross Ice Shelf was carried out during the 1996–1997 field season to characterize the morphology of naturally occurring snow ripples, a morphology that could be compared to ripple features in other sediments and would provide a data set against which numerical snow-surface feature simulation models could be validated. Snow-surface features were characterized using a new technique that involved capturing ripple cross-section shapes in digital images in the field for later analysis.

Snow-surface feature measurements were made adjacent to the Willie Field automatic weather station (AWS) (77.85°S 167.08°E) between 3 and 5 December 1996. The field team members responsible for these measurements were J. Stewart and C. Bennett. The features were characterized soon after a precipitation period that was associated with high wind speeds. The snow surface features observed were primarily transverse features (aligned perpendicular to the prevailing winds) such as snow ripples that were produced by winds 24 to 48 hours prior to the field measurements in the range of 8 and 14 meters per second. The basic sampling technique used in this investigation was initially devised by Werner et al. (1986) to characterize sand ripples.

This technique requires an apparatus (figure) consisting of a metal straight edge (on which is mounted a bubble level), a ruler, and a short post on the end of the apparatus. The straight edge is suspended above the snow surface by two

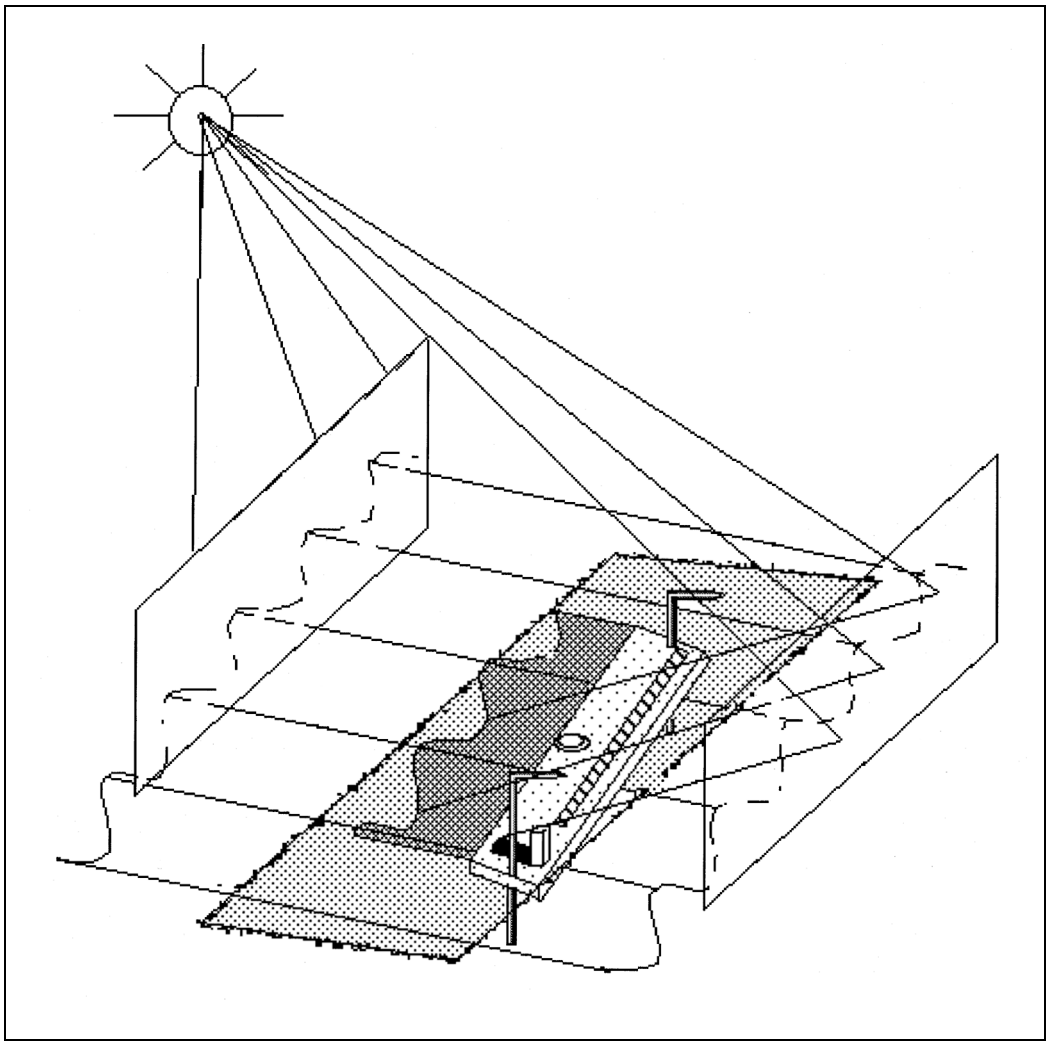

Schematic diagram of the apparatus used to characterize snow surface ripples. The apparatus is based on a technique devised by Werner et al. (1986) to characterize sand ripples.

stakes, which keep the apparatus from disturbing the surface feature. For transverse features, it is possible to use the shadow cast by the straight edge (which appears as an inverse ripple with the ridge of the surface feature casting the smallest shadow and the trough of the feature casting the largest shadow) to make accurate measurements of the feature. The shadow is cast by sunlight directed by a mirror perpendicular to the snow surface feature and apparatus. The length of the shadow cast by the small post on the straight edge is used to calculate the angle of the incident light (about 45 degrees). The angle is required to correct the surface-feature measurements using simple trigonometric relationships.

Images of the shadows were recorded digitally for later analysis using a Canon RC-250 still videocamera. The table summarizes the digital images obtained and the features characterized adjacent to the Willie Field AWS. Each digital image includes two internal calibrations: a scale, which enables the calibration of image pixels to centimeters, and the shadow length from the small post of known height, which allows the angle of the incident light to be calculated.

Images were later downloaded from the camera floppy disk to a Macintosh computer in the Crary Lab and analyzed using the public domain software package "NIH Image." NIH Image is a public domain image analysis program written by Wayne Rasband at the U.S. National Institutes of Health and is available over the Internet by anonymous file transfer protocol from *codon.nih.gov/pub/nih-image*. Image analysis techniques and corrections for the angle of the incident light using simple trigonometric relationships allowed surface-feature characteristics such as amplitude, wavelength, and length and angle of upwind and downwind slopes to be quantified with precision.

Two types of indices were determined for the surface features: a symmetry ratio, which is determined by dividing the windward portion of the wavelength by the leeward portion, and ripple ratio, which is determined by dividing the total wavelength by the ripple height. Because the partial upwind side and lee side wavelengths were measured independently of the total wavelength, a comparison of their sum to total wavelength was used to check the effect of image quality and operator skill on the data. Neither factor had a significant effect, suggesting the technique is both reliable and requires little practice. The projection ratio was found to be roughly the same for the two sampling days with mean values of 14.7 and 14.8. The symmetry ratio was found to have a larger difference in the mean values for the two sampling days with values of 0.353 and 0.451. The presence of the heightened

Digital images obtained and the features characterized adjacent to Willie Field AWS during the study period

Date	Digital images	Surface	Description
3 December 1996	31	35	Ripples
3 December 1996	6	1	Bedform under ripples
5 December 1996	79	133	Ripples

ridge of the surface features did not significantly influence either index.

This research was supported by National Science Foundation grant OPP 94-17255

References

Anderson, R.S., and B. Hallet. 1986. Sediment transport by wind: Toward a general model. *Geological Society of America Bulletin*, 97, 523–535.

Kobayashi, S., and T. Ishida. 1979. Interaction between wind and snow surface. *Boundary-Layer Meteorology*, 16, 35–47.

Kosugi, K., K. Nishimura, and N. Maeno. 1992. Snow ripples and their contribution to the mass transport in drifting snow. *Boundary-Layer Meteorology*, 59, 59–66.

Pomeroy, J.W., and D.M. Gray. 1990. Saltation of snow. *Water Resources Research*, 26(7), 1583–1594.

Schmidt, R.A. 1986. Transport rate of drifting snow and the mean wind speed profile. *Boundary-Layer Meteorology*, 34, 213–241.

Tufillaro, N.B., T. Abbott, and J. Reilly. 1992. *An experimental approach to nonlinear dynamics and chaos*. Redwood City, California: Addison-Wesley.

Waddington, E.D., J. Cunningham, and S.L. Harder. 1996. The effects of snow ventilation on chemical concentrations. In E.W. Wolff and R.C. Bales (Eds.), *Processes of chemical exchange between the atmosphere and polar snow* (NATO ASI Series I). Berlin: Springer-Verlag.

Werner, B.T., P.K. Haff, R.P. Livi, and R.S. Anderson. 1986. Measurement of eolian sand ripple cross-sectional shapes. *Geology*, 14, 743–745.

Characterization of snow accumulation variability on the Ross Ice Shelf, Antarctica

DAVID A. BRAATEN, *Department of Physics and Astronomy, University of Kansas, Lawrence, Kansas 66045*

Snow accumulation in a windswept area on the Ross Ice Shelf was investigated between November 1995 and November 1996 at a site adjacent to Ferrell automatic weather station (AWS) (78.02°S 170.80°E). The AWS provided this project with measured meteorological parameters such as wind speed, wind direction, temperature, and relative humidity (Holmes, Stearns, and Weidner 1993) at 10-minute intervals. The Ferrell AWS site has a wind regime that is frequently influenced by strong katabatic outflow winds from the Transantarctic Mountains. These winds make the site very suitable to study the role of winds on snow accumulation. More than 44 percent of the wind-speed observations exceed 5 meters per second (m s^{-1}), which is approximately the threshold wind speed for snow transport by wind. This site also has a dominant wind-direction corridor from 210° and has little directional variability for wind speeds greater than 5 m s^{-1} as shown by the wind rose in figure 1.

Snow-surface height was measured with a time resolution of 1 hour using a SR50 acoustic-ranging sensor, and the data were stored by a CR10 datalogger on a SM192 data-storage module (Campbell Scientific, Inc.). The data were recovered from the field at the end of the study period. The SR50 has a field of view of approximately 22° and measures the distance to the closest object within this field of view (e.g., the top of a snow-surface feature) with an accuracy of ±10 millimeters.The sensor was initially positioned approximately 1.4 meters (m) above the snow surface, and snow accumulation was calculated as the original distance of the SR50 sensor to the surface minus subsequent measured distances. The data-recovery percentage during the deployment period was more than 99 percent.

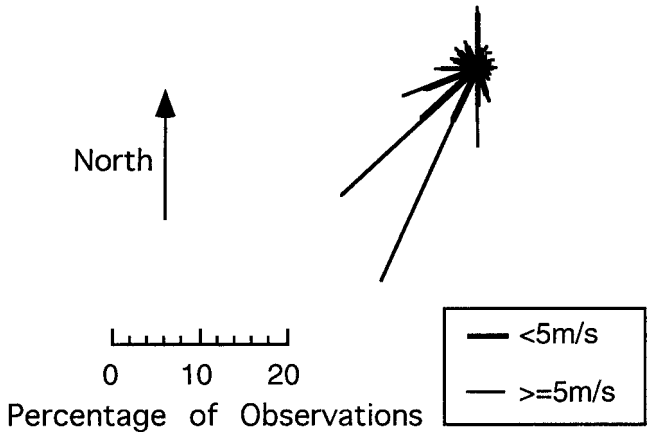

Figure 1. Wind rose for Ferrell AWS showing a dominant wind direction corridor with winds greater than 5 m s^{-1} blowing from around 210° with little directional variability. (m/s denotes meters per second.)

After quality-control checks of the data, a daily mean snow accumulation was calculated, and these data for the 12-month deployment are shown in figure 2. The acoustic snow-depth gauge shows four main snow-surface height increases ranging from about 5 centimeters (cm) to more than 20 cm, all occurring before 1 June 1996. These positive snow-surface height changes may be associated with precipitation, wind-blown transport of snow into the target area, and/or the formation of a surface feature on the target area. Because the winds during these periods are generally greater than the threshold speed for wind-blown snow (approximately 5–6 m s^{-1}), it is not known if the snow accumulation is due to precipita-

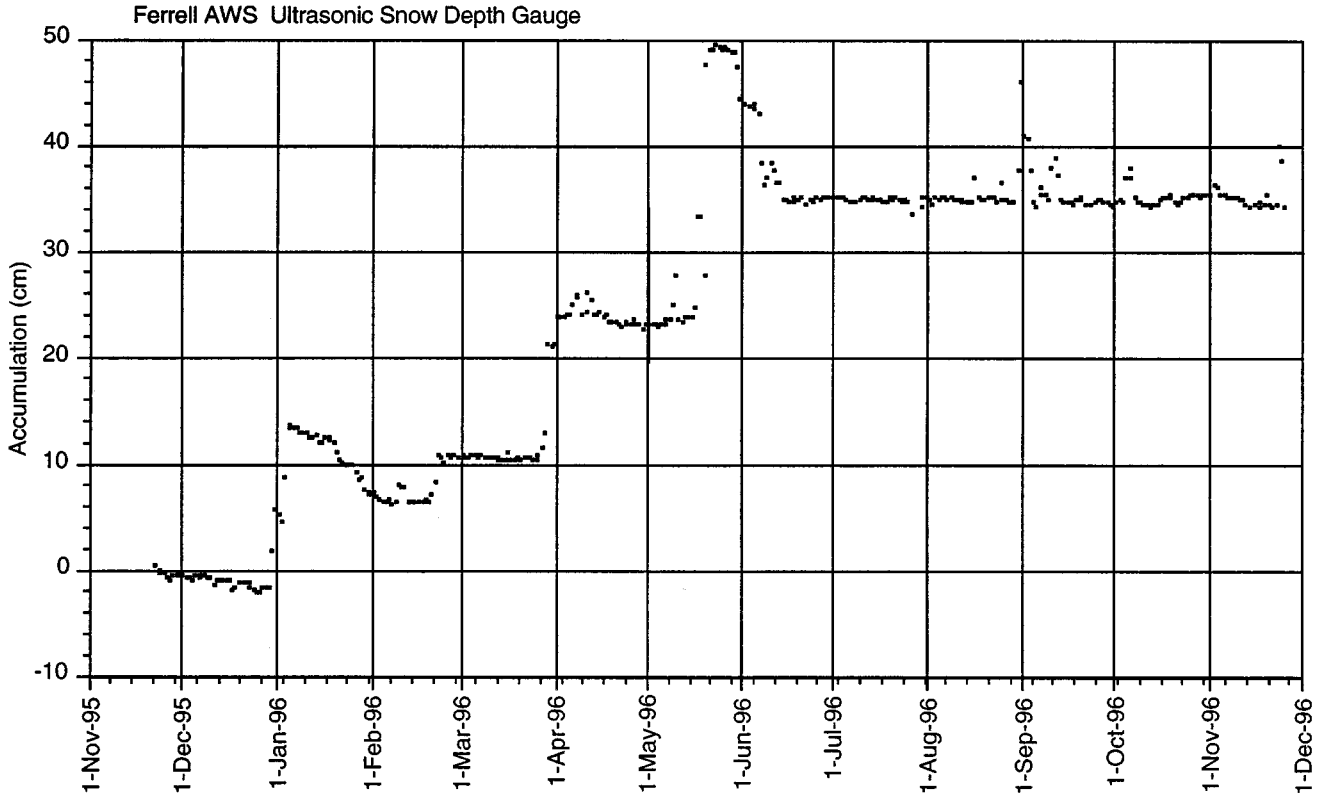

Figure 2. Daily mean snow accumulation at Ferrell AWS for the 12-month period between November 1995 and November 1996.

tion, wind-blown snow, the formation of a surface feature, or some combination of two or more of these processes. The acoustic snow-depth gauge also shows two large decreases (–8 and –15 cm) in snow-surface height occurring over several weeks after a large snow-surface height increase. Negative changes to surface height could have been caused by wind erosion of surface snow grains, sublimation at the snow surface, and/or metamorphic changes and densification of the firn.

During the 1996–1997 antarctic field season, Ferrell AWS was visited to conduct pit sampling and to retrieve the SR50 acoustic-ranging sensor data. The two field team members were D. Braaten and S. Seunarine. Three snow pits were sampled at 6, 12, and 16 m from the SR50 acoustic-ranging sensor in the prevailing downwind direction. The primary goal of the snow-pit sampling was the recovery of glass microspheres dispersed throughout the study period by the microsphere dispersal system (MDS) (Braaten 1994, 1995), but this sampling also provided a detailed snow-density profile and allowed the position of visual statigraphy observed along the snow-pit wall to be measured. The MDS was collocated with the SR50 acoustic-ranging sensor. Snow density was measured with a 1-cm resolution using disposable cuvette sampling tubes. Cuvette tubes were pushed into the snow-pit wall to obtain the snow sample, and snow density was determined by measuring the snow volume and water volume in the cuvette after melting. Results from the three snow pits are shown in figure 3. The snow-density profiles all have similar features, but these features can vary in depth by several centimeters. In each of the snow pits, six thin crust or glaze layers were visually identified, but it is not clear if these layers all correspond to the same time period. From the locations of microspheres recovered from the snow pits and SR50 acoustic-ranging sensor data, research is ongoing to date to explain the crust layers and to characterize the variability of snow accumulation on this temporal and spatial scale.

Other tasks performed during the 1996–1997 antarctic field season were removal of the MDS and SR50 acoustic-ranging sensor from Ferrell AWS, installation of this equipment adjacent to Marilyn AWS (79.954°S 165.130°E), and servicing of the MDS and SR50 acoustic-ranging sensor system at AGO-2 (85.67°S 46.38°W) on the polar plateau during the annual automatic geophysical observatory service visit.

This research was supported by National Science Foundation grant OPP 94-17255.

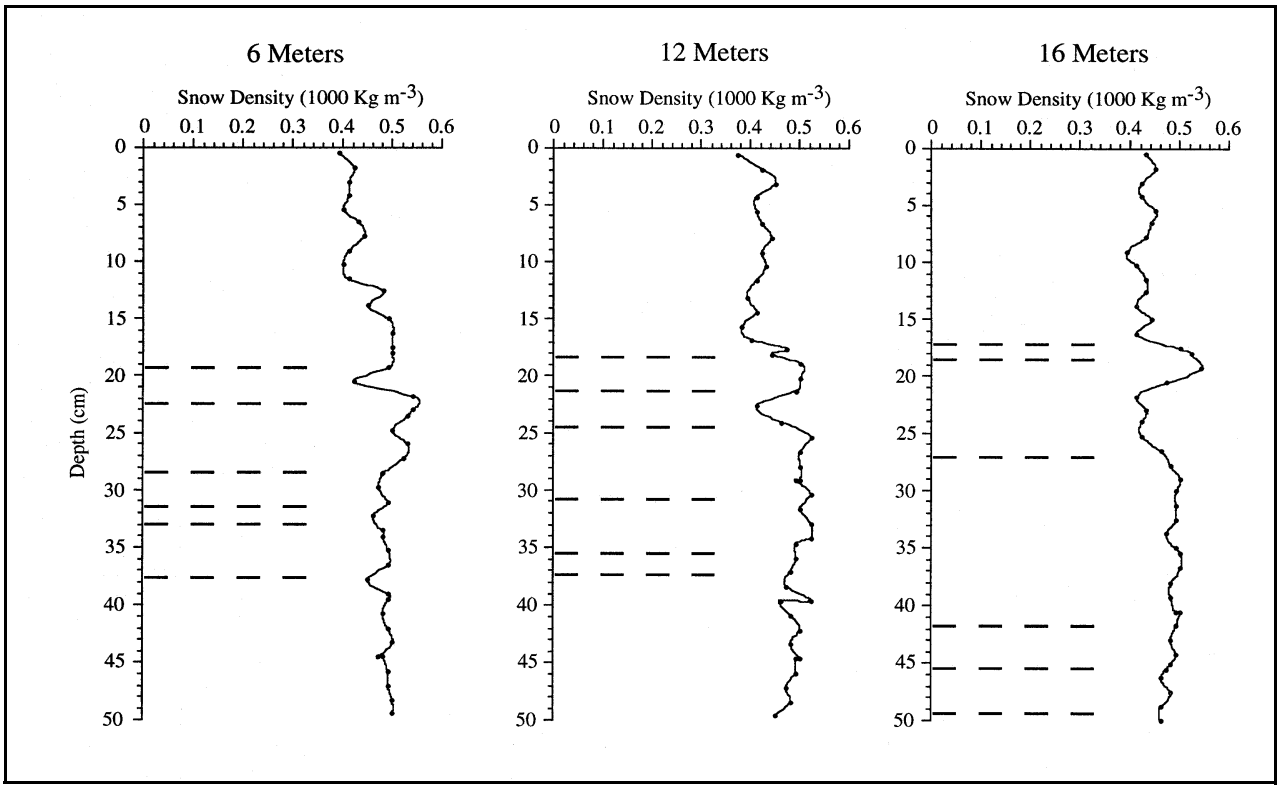

Figure 3. Detailed snow-density profile and visually observed crust layers in three snow pits located 6, 12, and 16 m from the SR50 acoustic-ranging sensor in the prevailing downwind direction. (Kg m^{-3} denotes kilograms per cubic meter.)

References

Braaten, D.A. 1994. Instrumentation to quantify snow accumulation and transport dynamics at two locations on the Ross Ice Shelf. *Antarctic Journal of the U.S.*, 29(5), 86–87.

Braaten, D.A. 1995. Assessment of snow accumulation and transport dynamics using glass microspheres. *Antarctic Journal of the U.S.*, 30(5), 331–332.

Holmes, R.E., C.R. Stearns, and G.A. Weidner. 1993. Antarctic automatic weather stations: Austral summer 1992–1993. *Antarctic Journal of the U.S.*, 28(5), 296–299.